



**CGU HS Committee on River Ice Processes and the Environment**  
17<sup>th</sup> Workshop on River Ice  
*Edmonton, Alberta, July 21 - 24, 2013*

---

**Analyses of 2011-2012 Four-Frequency Peace River AZFP Data**  
**M. Jasek<sup>1</sup>, J.R. Marko<sup>2</sup> and D.R. Topham<sup>2</sup>**

<sup>1</sup>*BC Hydro., Burnaby, BC, Martin.*  
*Jasek@bchydro.com*

<sup>2</sup>*ASL Environmental Sciences Inc., 6703 Rajpur Place Victoria, BC, V8M 1Z5*  
*[jmarko@aslenv.com](mailto:jmarko@aslenv.com); [dtopham@aslenv.com](mailto:dtopham@aslenv.com)*

A four-frequency AZFP (Acoustic Zooplankton Fish Profiler) instrument was deployed in the Peace River during the November, 2011-May, 2012 period near Town of Peace River. The deployment site was identical to that associated with previous deployments of one and two-frequency SWIPS (Shallow Water Ice Profiling Sonar) instruments. Acoustic volume backscattering coefficient and ice thickness data were collected at frequencies 125 kHz, 235 kHz, 455 kHz and 774 kHz. Backscattering coefficient data were acquired at 1 sec intervals as a function of height in the water column above the AZFP instrument. Initial analyses were carried out primarily on data collected during frazil formation intervals prior to stabilization of a stationary ice cover at the deployment site. This emphasis facilitated data processing within the particle size and concentration restrictions identified in a recent laboratory study of backscattering in pseudo-frazil suspensions (Marko, Topham, and Buermans, preceding presentation). The obtained results documented the changes occurring during frazil production intervals both as a function of time and as a function of vertical position in the water column. Changes in fractional ice volume and particle size distribution were quantified as a basis for model development and evaluation. The data were also used to explore alternatives for optimizing multi-frequency frazil characterization accuracy.

## 1. Introduction

The foregoing paper (Marko and Topham, 2013) described use of Acoustic Backscattering Sonar (ABS) laboratory data gathered on pseudo-frazil targets to validate use of similar techniques for characterizing real frazil populations. The next step in realizing the latter goal requires applications to actual ABS field data, with such applications directed at utilizing measurements at, three or more acoustic frequencies to both verify the effectiveness of the outlined approach and explore possibilities for loosening restrictions imposed by the limitations of the laboratory testing. The work described below carries out these tasks through use of data acquired by BC Hydro on the Peace River in the period Nov., 2011-April, 2012 at four acoustic frequencies similar to those utilized in the laboratory work. Focus in the analyses is given to data acquired in periods both preceding formation of a local ice cover and late in the ice covered season when the relative absence of overhead floating ice allowed comparisons with thermal frazil growth models.

## 2. Methodology

### 2.1 Measurement framework and instrumentation

The analysis framework assumes the availability of volume backscattering coefficient,  $S_v$ , time series data at, at least, two frequencies. Theoretical values for these coefficients, which essentially represent the fraction of acoustic power incident on a unit volume of suspended targets which is scattered directly back toward the source, can be written as:

$$S_v^{\text{Theo}}(v_i) = N \int_0^{\infty} g(a_e) \sigma_{bs}(a_e, v_i) da_e \quad [1]$$

In this equation  $N$  denotes the total number of particle targets/unit volume;  $a_e$  is the effective radius of a given particle;  $\sigma_{bs}(a_e, v_i)$  is the backscattering cross section of such a particle at the acoustic frequency  $v_i$  and  $g(a_e, b)$  satisfies:

$$\int_0^{\infty} g(a_e) da_e = 1. \quad [2]$$

There are good theoretical reasons, confirmed by lab testing (Clark and Doering, 2006), for assuming that  $g(a_e)$  can be expressed as a two parameter lognormal distribution:

$$g(a_e, a_m, b) = \left[ (2\pi)^{0.5} b a_e \right]^{-1} e^{-\{0.5(\ln(a_e/a_m)/b)^2\}}. \quad [3]$$

with the two additional parameters being:  $a_m$  which is the median value of the effective radii; and  $b$  as a determinant of radius variance or “spread”. As in past usage (Ashton, 1983; Marko and Jasek, 2010a,b) the effective radius is defined as the radius of a sphere with a volume equal to that of a given particle.

The main purpose of the “framework” developed in the preceding paper (Marko and Topham, 2013) was to identify measurement situations for which we can safely assume both the applicability of Equation 1 and the availability of similarly reliable knowledge of the individual backscattering cross section relationship  $\sigma_{bs}(a_e, v_i)$ . In the first case, this involved establishing particle radius-dependent upper limits on particle concentration,  $N$ , to avoid effects from coherence, attenuation and other sources which undermine the independent scattering assumption. Estimates in this regard appeared to show sensitivity was primarily attributable to the larger particles present and suggested that Equation 1 was likely to retain validity for overall concentrations well above  $10^7/\text{m}^3$ . Equivalent confidence in  $\sigma(a, v_i)$  relationships required estimating the domains of applicability for the Anderson (1950) multipolar expansion which can be written in terms of modal series coefficients,  $b_m$ , (Stanton et al., 1998) as:

$$\sigma_{bs}(a_e, v) = (\pi a_e^2/4) \left| \left( \frac{i}{k_1} \right) \sum_{m=0}^{\infty} b_m (-1)^m \right|^2. \quad [4]$$

When expressed in terms of effective radii, the laboratory results suggested that Equation 4 was closely representative of individual cross sections for combinations of  $v = v_i$  and  $a_e$  which satisfy  $2\pi v_i a_e / c \leq 0.7$ , where  $c$  denotes the speed of sound in the fluid medium and  $v_i$  is the acoustic measurement frequency.

Given the availability of measurements of volume backscattering coefficients  $S_v^{\text{meas}}(v_i)$  at 3 different frequencies, the minimum of the sum of squared differences between measured and theoretical values:

$$q = \sum_{i=1}^{i=3} \left[ \langle S \rangle_v^{\text{meas}}(v_i) - S_v^{\text{Theo}}(v_i) \right]^2, \quad [5]$$

can be used to derive values for  $N$ ,  $a_m$  and  $b$  which provide all the information needed to optimize agreement between measured and theoretical  $S_v$  values. This information allows the numbers of particles/unit volume to be characterized as a function of effective radius as:

$$dN = N g(a_e, a_m, b) da_e. \quad [6]$$

The fractional ice volume conventionally used in river frazil characterizations can be derived from the optimized population parameters through, respectively:

$$F = N \int_0^{\infty} (4\pi/3) a_e^3 g(a_e, a_m, b) da_e \quad [7]$$

Likewise, corresponding frazil disk face diameters can be obtained by multiplying  $a_e$  by factors of 3.7 or 4.25 according to one’s respective preferences for 10:1 or 15:1 as ratios of typical disk diameter to thickness.

Data suitable for applications and testing of this measurement framework were obtained between November, 2011 and April, 2012 by BC Hydro at its annual monitoring site near Town of

Peace River, Alberta. Data acquisition utilized a 4 frequency Shallow Water Ice Profiling Sonar (SWIPS) unit (manufactured by ASL Environmental Sciences Inc.) which operated at frequencies of 125 kHz, 235 kHz, 455 kHz and 774 kHz from four adjacent bottom-mounted, upward-looking, transducers in water depths of about 5 m. This instrument was closely similar to the AWZFP used in the above-described (Marko and Topham, 2013) laboratory studies with the exception of the latter instrument's use of slightly different frequencies in two channels (200kHz vs. 235 kHz and 769 kHz vs 774 kHz) and its inclusion of logarithmic signal detection. Individual pulses and returns were emitted and detected in each frequency channel at 1 Hz. Averaging over 2 adjacent (in time) voltage samples returned measures of backscattering from 4 cm range cells.

## **2.2 Deployment and Field conditions**

The upstream advance of the Peace River ice cover toward the Town of Peace River deployment site during the 2011-2012 winter was very close to being historically slow (Figure. 1). Specifically, the upstream ice edge reached the instrumented site in mid-February and only began to advance more than a few km further upstream in March. At the time of maximal advance, barely 20 km of ice lay upstream of the site which, except for very brief incursions, became largely ice-free after March 15. These conditions were almost ideal for studies of “active” frazil formation (Martin, 1983) during several intervals of prolonged supercooling which both preceded the local arrival of the ice edge and, to a lesser extent, which followed ice edge retreat.

## **3. SWIPS Results**

### **3.1 Data selection and analysis goals**

Random subsamples of the acoustic return profile records together with reviews of seasonal air temperature, and ice condition survey data were used to identify time intervals likely to have been associated with active frazil ice at the monitoring site. Emphasis was given to acquiring data which included but was not restricted to short term and overall seasonal peaks in the frazil acoustic return strengths. Data were selected from five suitable intervals which from the period prior to arrival of the seasonal ice edge and, as well, from two other intervals which followed ice clearance. The latter intervals, because of higher spring solar energy fluxes were more strongly diurnal in character relative to their early season counterparts.

The analyzed intervals, listed in Table 1, provided approximately 101 hours of acoustic data in each frequency channel. About 85 hours of this total were coincident with the largely ice-free conditions prevalent prior to Feb 12: corresponding to about 10 % of the predicted 774 hour total duration of frazil presence (see section 4) for this period.

Our analyses were directed at two main objectives:

- Clarifying the relative advantages/disadvantages for frazil characterizations of using data gathered at, alternatively, the lower and upper ends of the tested (125 kHz-774 kHz) range of acoustic frequencies; and

- Using data gathered with the resulting optimal suite of frequencies to document and assess the characteristics of “active” frazil ice at the Peace River monitoring site.

### 3.2 Acoustic Profiling Results

Since our characterizations involve 3 unknown parameters,  $N$ ,  $a_m$  and  $b$ , and included independent measurements at 4 acoustic frequencies, the first of the above objectives could be addressed through comparisons of parameters extracted using  $S_v$  data gathered, alternatively, in channels 1-3 (125 kHz - 455 kHz) or in channels 2-4 (200 kHz - 774kHz). Distinctions then have to be made on the relative merits of the resulting data sets which differ only through the underlying inclusion of, alternatively, the highest or lowest available acoustic frequencies. Such judgements can be based upon both the general character and consistency of the results as well, more quantitatively, on the magnitudes of the squared theoretical and measured  $S_v$  values differences as represented by the  $q$  parameter (Equation 5). Actual extraction of optimal  $N$ ,  $a_m$  and  $b$  parameter triplets utilized ASL’s standalone RUNSWIPS software which converts raw backscatter signal voltages into values, averaged over user-specified time and range intervals and performs corresponding extractions. The resulting parameters can be used, through Eqs. 3 and 6, to estimate the numerical concentrations of particles in any particular range of effective radius,  $a_e$ , or equivalent disk diameter values and for calculating the fractional volumes which quantify water column ice content. Options are offered for processing either the averaged  $S_v$  values either “as is” or after subtraction of estimated non-frazil-related “backgrounds”. These background  $S_v$  levels can change from time to time, reflecting changes in water column sediment and the numbers and strength of other non-ice targets. Fortunately, these levels are almost always at least 10 dB below those associated with detectable frazil. Consequently, significant background impacts upon parameter extraction are limited to marginally detectable frazil populations which are typically characterized by large values of  $q$  and, hence, unreliable parameter extraction.

Observations (see below) that the temporal character of frazil backscattering shows, at best, only weak dependences on position in the water column. This allows many of the qualitative characteristics of frazil variability to be seen in  $S_v$  vs.  $t$  data gathered at common mid-water depths. Time series data of this type are plotted in Figure 2 for 7 studied time intervals and correspond to measurements made for cells centred at ranges of 2.3m for intervals 1-5 and 2.63 m for intervals 6 and 7 which were associated with slightly higher river water levels. In both cases the measurement ranges were about 2.7 m below the air-water interface.

The  $S_v$  vs.  $t$  curves are striking in their individual smoothness, similarity and, in particular, in the stability of channel to channel differences over extended periods. Peak levels among each of the depicted intervals tended to be within +/- 3dB of a channel-specific median value although, of course, variations as large as 20 dB were observed over time periods of a few hours usually associated with the definitive beginnings and terminations of frazil presence. The repeated prevalence of relatively constant gaps between adjacent curves during periods of smoothly changing  $S_v$  levels was particularly noteworthy: suggesting that the underlying changes were occurring primarily in numerical frazil particle concentrations. This conclusion reflects the fact that unchanging separations of logarithmically-plotted (Urlick,1984) backscattering coefficient values are indicative of constancy in the ratios of the corresponding non-logarithmic quantities represented theoretically by Equation 1. Such constancy is only likely in the absence of

significant changes in cross sections and, hence, in the particle dimensions which, at a given frequency, are the primary source of cross section variation. Conversely, less frequent widening or narrowing of such gaps can be tied to particle dimension changes. Examples of such changes were present in most studied intervals and tended to follow shortly upon occurrences of sudden jumps, decreases or temporary dips in  $S_v$ . These characteristics of the plotted curves suggest that a significant portion of local frazil variability arises from the successive passages of demonstrably different frazil populations: each sharing a relatively common size distribution and an internal gradient in overall particle concentration numbers. Other occasional features of the  $S_v$  vs.  $t$  curves, such as the anomalous drop at the end of the channels 4 curve in Figure 2g, require additional interpretations in terms of other factors such as acoustic beam blockage by anchor ice which preferentially attenuates higher acoustic frequencies.

While this simple interpretation of the data would appear to bode well for characterizing local frazil conditions from acoustic profiles, other aspects of the results in Figure 2 are indicative of needs for refining of our interpretative framework rules. Difficulties in these respects are most apparent in some of the channel 1 data: with particular concerns arising from occasional near equalities in channel 1 and 2  $S_v$  values. Calculations based upon Equation 4 suggest that “cross-overs” can occur in these channels but, only for values of  $a_e$  approaching unity. As will be seen below, such large values of  $a_e$  were extremely unlikely to have been prevalent during the studied intervals. Consequently, the observations of anomalously small gaps between the channel 1 and 2 curves were suggestive of tentative, confirmation of earlier observations (Marko and Topham, 2013) of similarly anomalous higher than expected channel 1  $S_v$  values. As in that case, the most likely origins of these results were anticipated to be attributable to additional scattering contributions from fluid turbulence targets.

All parameter extractions were derived from  $S_v$  data averaged over 20 cm segments of the water column centred at 4 different representative ranges extending from, roughly, 1m above the plane of the transducer faces to 0.7 m below the river surface. Interpretation of the RUNSWIPS-processed results was facilitated by side-by-side displays of parameters corresponding to successive representative ranges. Such displays are presented in Figures 3a,b and 4a,b both to illustrate the basic characteristics of analysis output and as a basis for addressing the first of the two above study objectives. The plots in each figure, reading from top to bottom, depict values of  $F$ ,  $N$ ,  $q$ ,  $a_m$  and  $b$  for individual averaging intervals. The fractional volume  $F$ , as noted above, was derived from the extracted values of  $N$ ,  $a_m$  and  $b$ . The quantity  $q$  provided a quantitative measure of the quality of individual extractions. Figures 3 and 4 are, respectively, representative of Jan.2-3 and Feb.6-Feb.7 measurements (intervals 2 and 5 in Table 1) based upon data gathered in, alternatively, channels 1-3 (Figures 3a and 4a) and channels 2-4 (Figures 3b and 4b). In all cases, parameter values were only plotted when corresponding values satisfied the inequality  $q < 50$ . This restriction pretty much eliminated wildly inaccurate extractions (since mean differences between theoretical and measured  $S_v$  values are approximately given by  $(q/3)^5$ , a  $q$  of 50 corresponded to roughly 4 dB differences in each channel). Such data points were almost always associated with 10 minute averaging periods corresponding to negligible, weak or erratic frazil backscattering. Whenever possible analyses focused on data acquired with  $q \leq 12.5$ , corresponding to average channel theory/measured discrepancies of 2 dB or less. As will be seen, extraction quality usually well exceeded even this level except during periods of marginal frazil detectability.

Inspections of the data in Figures 3 and 4 are indicative of the higher quality of the parameters extracted in channels 2-4 although, in both intervals, credible and, roughly, comparably-sized parameter values were derived for both channel combinations with acceptable values of  $q$ . Nevertheless, the higher  $q$  values and more erratic parameters noted in the channel 1-3 results are readily distinguishable relative to lower  $q$ 's and more consistent results obtained with channel 2-4 data. In fact, the latter results (Figures 3b and 4b) suggest that, for times coincident with significant frazil presence, the mean rms differences of  $S_v^{\text{Meas}}(v_i) - S_v^{\text{Theo}}(v_i)$  in individual channels are on the order of or less than 1 dB. Such differences correspond to levels of agreement comparable to or better than achieved in our single species pseudo-frazil measurements (Marko and Topham, 2013) and fall within the  $\pm 1$  dB uncertainties of individual channel calibrations. These results (supported by data gathered during all other tested intervals) strongly suggest that channel 1 data are contaminated by returns from non-frazil sources which undermine accurate interpretation in terms of our framework. In other words, the inaccuracies introduced by turbulence-related scattering at 125 kHz exceed those arising at 774 kHz from possible violations of the spherical target assumption underlying Equation 4. More quantitatively, using the largest, 0.3 mm, median  $a_e$  values ( $a_m$ ) extracted and displayed in Figures 3b and 4b, to conclude the spherical target assumption would appear to retain validity for values of  $k_1 a_e$  at least as high as 1.04. This is well above the 0.7 limit deduced from the pseudo-frazil measurements.

Resolution of the frequency selection issue allowed use of Figures 3b and 4b as a basis for drawing initial impressions of Peace River frazil characteristics during two, relatively short, mid-winter frazil growth intervals. Reviews of the parameter values extracted for times associated with low  $q$  values confirmed the general patterns of variability deduced above on the basis of the  $S_v$  vs.  $t$  curves of Figure 2. Specifically, changes in fractional volume closely tracked variations in particle concentration,  $N$ , with median particle effective radii,  $a_m$  varying between 0.25 and 0.30 mm during the January 2-3 interval and between 0.20 and 0.25 mm on February. 6-7. Mid-water concentrations of particles as functions of effective radius at times of peak fractional volume are plotted in Figure 5 as calculated using values of  $a_m$  of 0.28 mm and 0.23 mm and corresponding "spread" parameters,  $b$ , of 0.15 and 0.1, respectively. These results are indicative of relatively narrow spreads of particle dimensions around median values: suggesting that backscattering contributions from particles large enough to have cross sections incompatible with Equation 4 can be safely ignored.

It is notable that fractional volume peaking events in Figures 3b and 4b, which corresponded to values of  $4 \times 10^{-5}$  and  $5.5 \times 10^{-5}$ , occurred shortly after the initial sharp rise in frazil presence. Similar timings of maximal fractional volume were observed in all but one of the studied intervals. This feature of the studied event may reflect successions of widespread local growth followed by observations of slowly diminishing concentrations advected from areas much further upstream.

Much less uniformity was evident in the depth/range dependences of fractional volume. Specifically, the significant progressive increases in  $F$  with height in the water column so apparent in the January 2-3 and February 6-7 intervals were only evident throughout the course of one other studied interval (March 22). Three of the four remaining intervals showed either

negligible or much smaller changes in  $F$  and other population parameters as a function of height in the water column with the possible exception of the highest (longest range) measurement level where surface ice may have been present. This situation is illustrated in the results from the January 14-15 and January 25-26 intervals (Figures 6 and 7). These two intervals corresponded to the beginnings of two immediately adjacent and prolonged periods expected, from current ice growth models, to be characterized by the nearly continuous presence of frazil ice. The first of these intervals, represented by slightly less than 30 hours of January 14-25 data, was associated with the largest fractional volumes detected in the water below our uppermost extraction ranges (4.27 m and 4.49 m). The actual peak fractional volume,  $1.6 \times 10^{-4}$ , was associated with the first of 5 peaking events associated with this interval (Figure 2c) and corresponded to ice contents 2 to 8 times larger than mid- and lower-water column peaks observed during, with one exception, all other intervals. That exception was the post-clearance March 22 interval which included peak values of  $1.2 \times 10^{-4}$ .

Searches for the origins of these two different kinds of behavior: i.e. fractional volumes which, alternatively, do and do not significantly increase with height in the water column, are suggestive of two possible correlants:  $q$  and  $a_m$ . In the first case,  $q$  values associated with extractions in the presence of strong vertical gradients in intervals 2, 5 and 7 tended to be below 5 (Figures 3b and 4b) while the more uniformly distributed fractional volumes of intervals 1, 3 and 4 were extracted, more typically, with larger  $q$  values extending up 15 and higher. Correlations with extracted mean effective radii, on the other hand, seemed to link the presence and absence of vertical fractional volume gradients in  $F$  with values of  $a_m$  alternatively larger and smaller than 0.2 mm. Although, clearly, our data are still too few in number to confirm such fine distinctions it is interesting to note that interval 6 exhibits (Figure 8) both kinds of behavior with vertical gradients being associated with the fractional volume peak at the beginning of the interval and height independence in evidence afterwards. In both cases, the dependence of  $F$  on height in the lower and middle water column appear to show the noted correlations with  $q$  and  $a_m$ .

These speculations reflect the continued presence of interpretative subtleties and puzzles in the acoustic data sets. Nevertheless, this presence should not obscure the strong evidence for both highly consistent (i.e. theoretical values reproducing measured values within measurement error) and somewhat less consistent (mean errors up to and beyond 2 dB) parameter extractions which, nevertheless, yield very similar ranges of values for  $F$  and other parameters. Tentative correlations with vertical gradients in particle numbers and fractional volume point toward explanations involving gradients in turbulent scattering and linkages to surface and suspended ice conditions and, possibly, other environmental factors. Some clarifications of this situation might be expected from processing additional portions of the 2011-2012 data sets.

It should be noted that the actual seasonal fractional volume maximum was observed at the end of November 20-21 interval when several 10 minute averaged values were in excess of  $2 \times 10^{-4}$  at a range of 4.27. This value and the accompanying extracted value of  $a_m = 0.35$  were closely similar to results obtained at the same range at the end of the January 14-15 interval (Figure 6). In both cases, detailed reviews indicated likely contamination of the 4.27 m cell return by surface ice (Figure 9). In the latter case, it can be seen that decreasing water levels also contributed to increasing the presence of surface ice at the 4.27 m measurement range.

### 3.3 Accuracy Issues

The utility of the obtained frazil characterization data and the underlying measurement and interpretative framework is, of course, heavily dependent upon their respective accuracies. Ultimately, assessments in these regards are likely to require simultaneous independent verifications by independent, non-acoustic, methodologies which could be as “simple” as weighing frazil volumes captured above an operating upward-looking SWIPS instrument. A previous attempt at such verifications (Ghobrial et al., 2012), carried out in a laboratory tank, was limited to the production of empirical relationships between  $S_v$  values measured at individual acoustic frequencies and  $F$ . Applications of such algorithms to actual field measurements requires (Ghobrial et al., 2013) an unproved assumption of identical laboratory and field frazil particle size probability distributions. Moreover, the resulting empirical algorithms were derived from measurements on frazil populations characterized by minimum fractional volumes (averaged over the water column) no lower than  $1.2 \times 10^{-4}$ . These origins in data acquired for fractional volumes which are much higher than inferred in our measurements make the empirical algorithm inapplicable to verifications of the 2011-2012 Peace River frazil characterizations.

Consequently, arguments for the validity of the characterizations have to be based upon the quality of the agreement achieved between values of  $S_v$  measured at 3 different frequencies and theoretical values obtained using Eqs. 1 and 4. Confidence in this approach is based upon its equally successful use in laboratory tests upon both single species and mixtures of pseudo-frazil disks with shapes and sizes closely approximating those inferred to be associated with the Peace River frazil disk populations. This verification draws upon the recognition that the applicability of Equation 1 has been validated within the frequency and size constraints identified in the pseudo-frazil tests (except, perhaps, for the Channel 4 data) and can be applied to the frazil particle in freshwater case by, merely, use of corresponding appropriate mass density and sound speed parameters. The inclusion of the channel 4 data in the validated category can be justified by the resulting close similarity of the extracted parameters with those obtained when the channel 4 data is replaced by data from the problematic channel 1. Although, clearly, field verification by independent, near simultaneous, measurements of fractional volume is recommended, in our view, the great weight of evidence from the laboratory and field frazil measurement programs is that the latter are now capable of specifying frazil population composition to realistic accuracies for river modelling and management purposes.

#### Acknowledgements

The authors wish to express their gratitude for Laura Simandl’s considerable contributions, in conjunction with David Billenness, to the development of the RUNSWIPS processing algorithm and for carrying out the tedious tasks of data selection and processing.

#### References

- Anderson, V.C., 1950. Sound scattering from a fluid sphere. *J. Acoust. Soc.* 22, 426-431.  
Ashton, G.D., 1983. Frazil ice. In: *Theory of Dispersed Multiphase Flow*. Academic Press N.Y., 271-289.

- Clay, C.S., Medwin, H., 1977. *Acoustical Oceanography*. Wiley-Interscience, New York.,544 pp.
- Ghobrial. T.R., Loewen, M.R., Hicks, F.E., 2012. Laboratory calibration of upward looking sonars for measuring suspended frazil ice concentration. *Cold Reg. Sci Technol.* 70, 19-31.
- Ghobrial. T.R., Loewen, M.R., Hicks, F.E., 2013. Characterizing suspended frazil ice in rivers using upward looking sonars. *Cold Reg. Sci Technol.* 86, 113-126.
- Marko, J.R., Jasek, M., 2010a. Sonar detection and measurements of ice in a freezing river I: Methods and data characteristics. *Cold Reg. Sci Technol.* 63, 121-134.
- Marko, J.R., Jasek, M., 2010b. Sonar detection and measurements of ice in a freezing river II: Observations and results on frazil ice. *Cold Reg. Sci. Technol.* 63, 135-153.
- Marko, J.R., Jasek,M., 2010c. Frazil Monitoring by Multi-frequency Shallow Water Ice Profiling Sonar (SWIPS): Present Status. *Proc. 20th IAHR International Symposium on Ice, Lahti, Finland.*
- Marko, J. R. and Topham, D.R., 2013. Laboratory measurements of backscattering from pseudo-frazil particles. *Proceedings of the 17<sup>th</sup> Workshop, Committee on River Ice Processes and the Environment. (Preceding paper).*
- Stanton, T.K., Wiebe, P.H. and Chu, D., 1998. Differences between sound scattering by weakly scattering spheres and finite-length cylinders with applications to sound scattering by zooplankton. *J. Acoust. Soc.* 103, 254-264.
- Urick, R.J. 1984. *Principles of Underwater Sound*. Peninsula Publishing, Los Altos, CA, 423 p.

## Tables

Table 1. Analyzed frazil intervals

Interval	Start and end times, dates	Duration (hrs)
1	17:14 Nov. 20 to 01:04 Nov 21	8
2	01:34 Jan.3 to 12:55 Jan.3	11
3	19:34 Jan 14 to 23:57 Jan 15	29
4	07:34 Jan.25 to 13:45 Jan.26	30
5	23:04 Feb 6 to 04:04 Feb. 7	5
6	02:04 Mar. 20-10:44 Mar. 20	8.5
7	00:44 Mar. 22 to 09:44 Mar. 22	9

## Figures

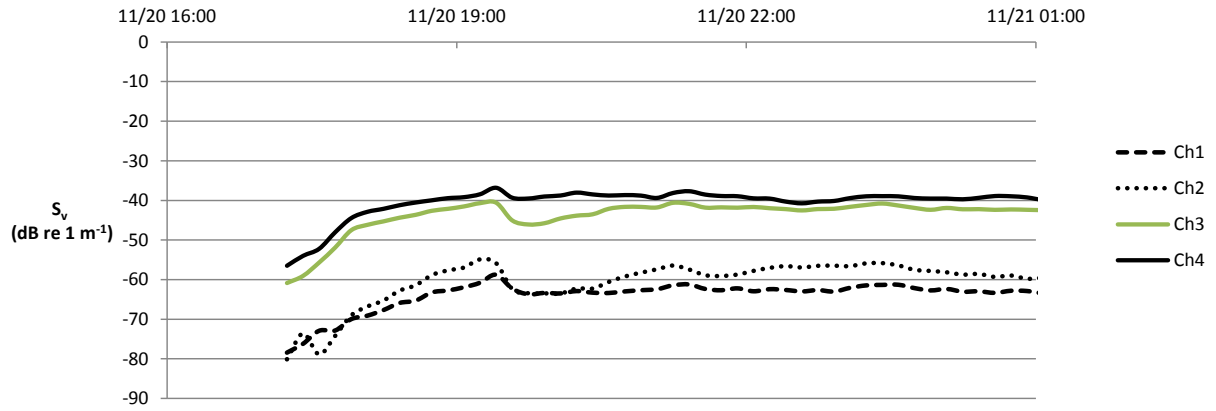


Figure 2a.  $S_v$  vs t results in channels 1-4 for frazil study interval 1.

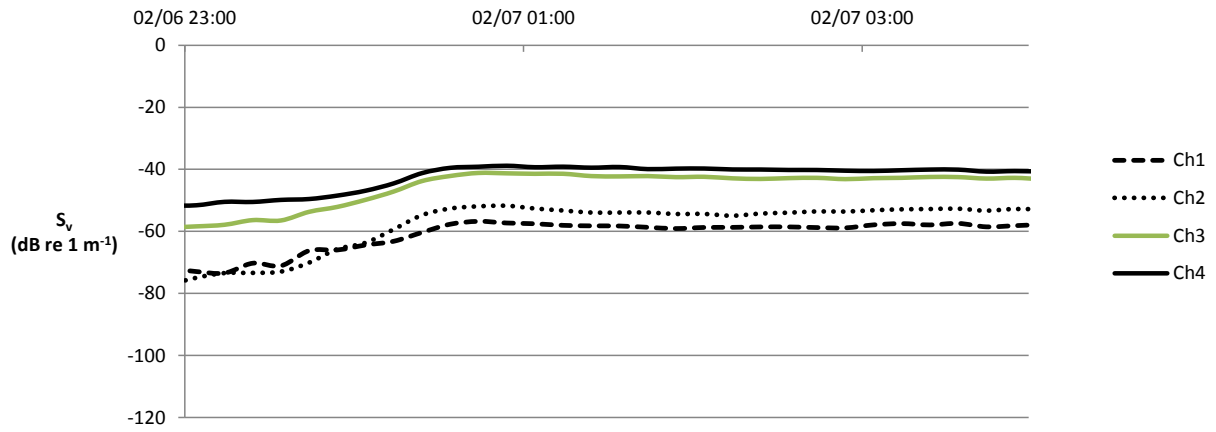


Figure 2b.  $S_v$  vs t results in channels 1-4 for frazil study interval 2.

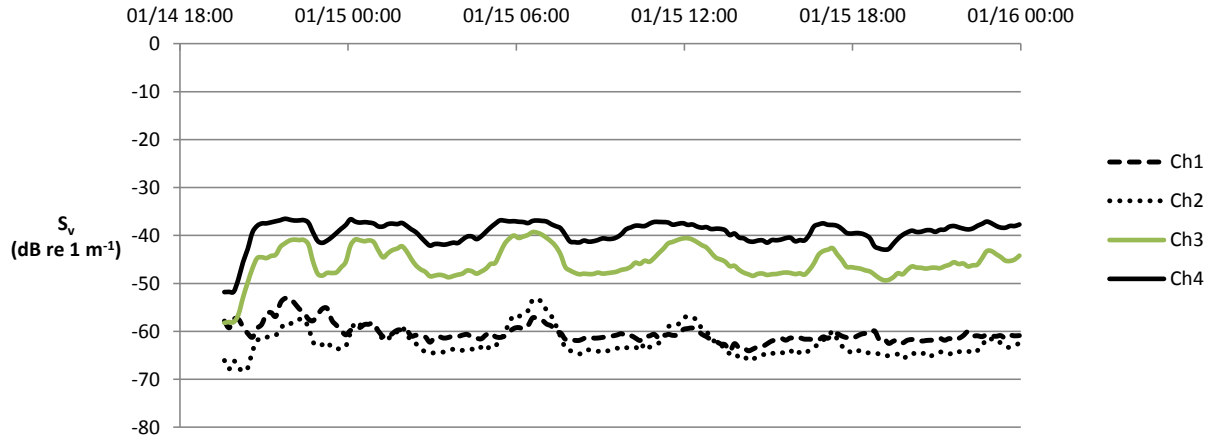


Figure 2c.  $S_v$  vs  $t$  results in channels 1-4 for frazil study interval 3.

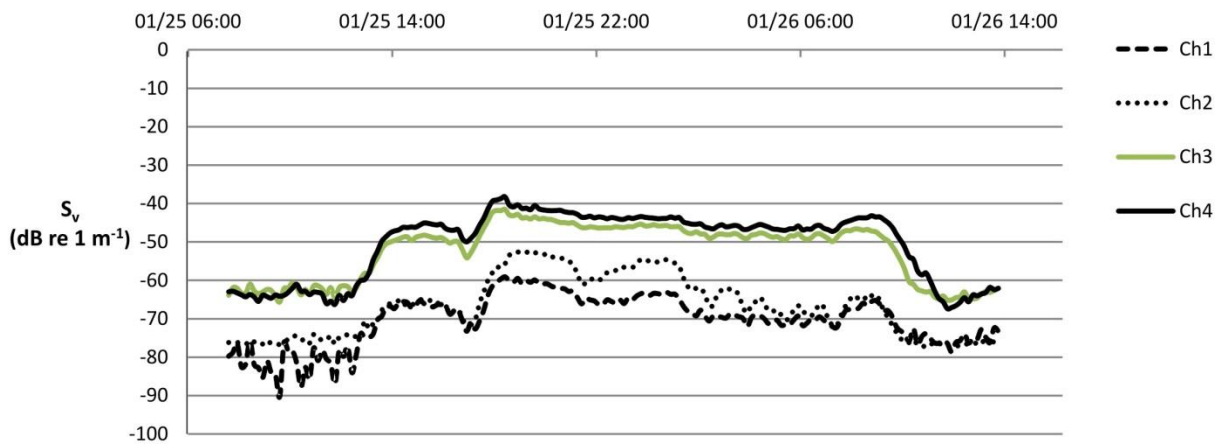


Figure 2d.  $S_v$  vs  $t$  results in channels 1-4 for frazil study interval 4.

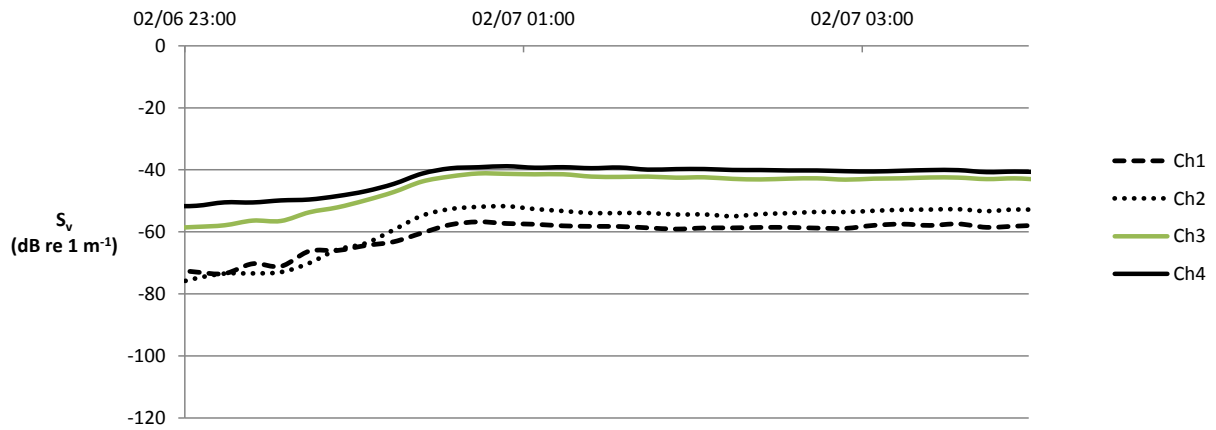


Figure 2e.  $S_v$  vs t results in channels 1-4 for frazil study interval 5.

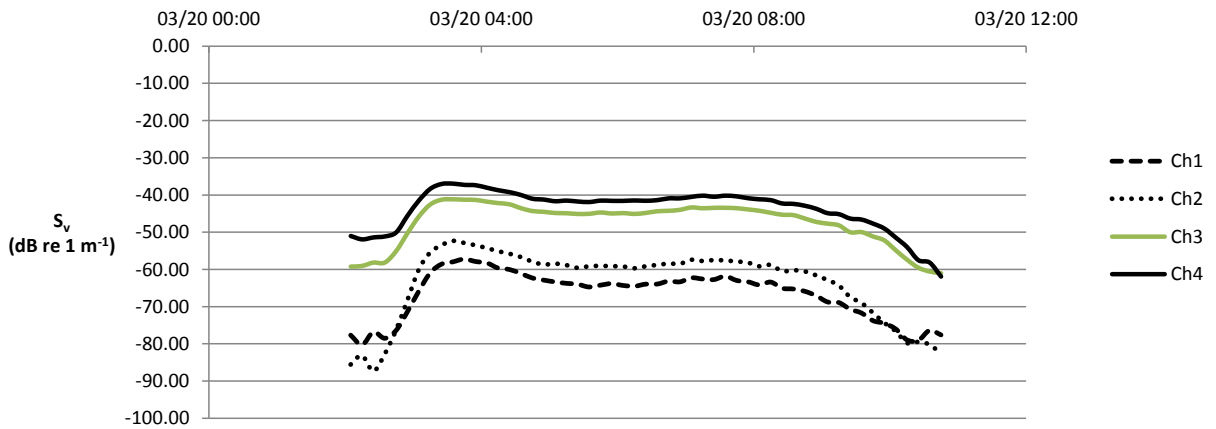


Figure 2f.  $S_v$  vs t results in channels 1-4 for frazil study interval 6.

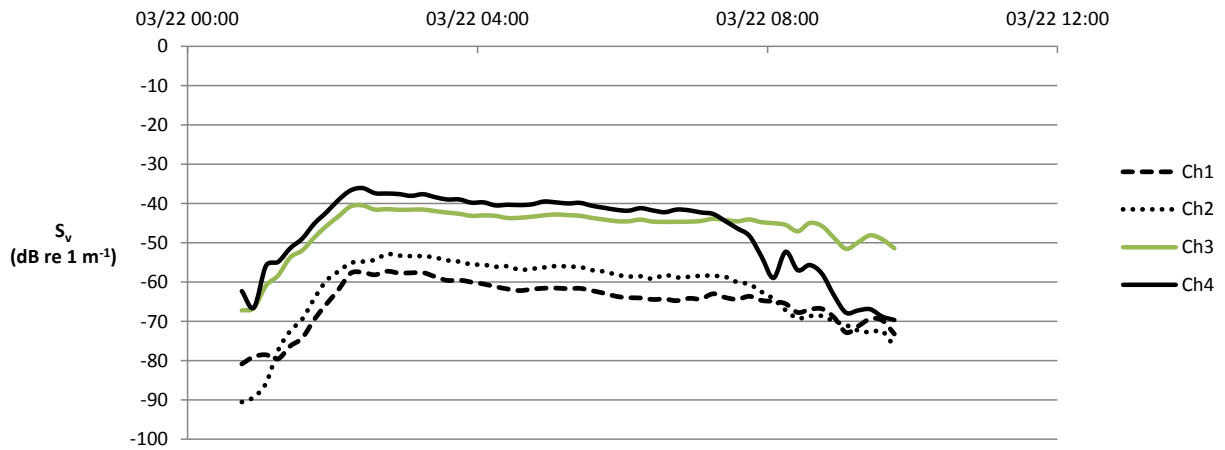


Figure 2g.  $S_v$  vs  $t$  results in channels 1-4 for frazil study interval 7.

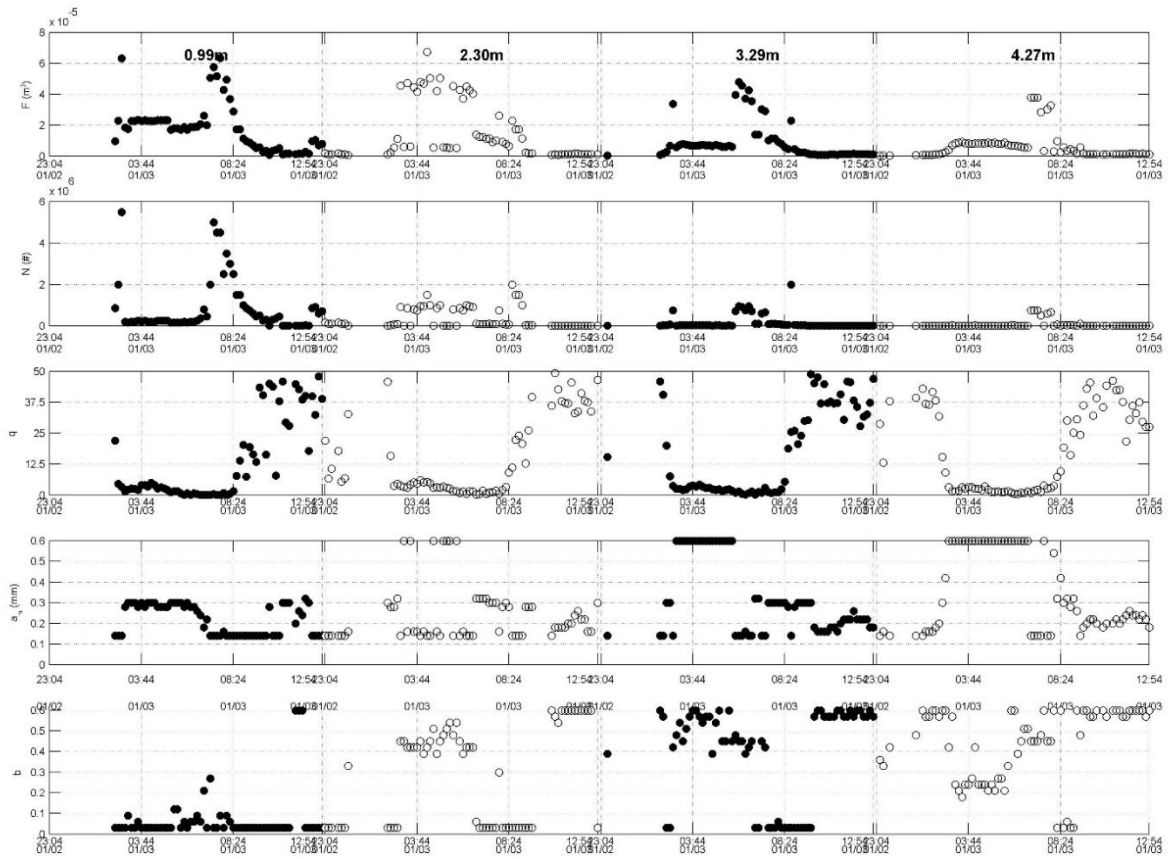


Figure 3a. Plots of extracted and derived parameters corresponding to 10 minute-averaged channels 1-3 data from interval 2. Reading from the top to the bottom of the Figure, the plotted quantities are:  $F$  (fractional volume);  $N$  (particle concentration (particles/ $\text{m}^3$ ));  $q$  (quality factor);  $a_m$  (median effective radius); and  $b$  (radius spread).

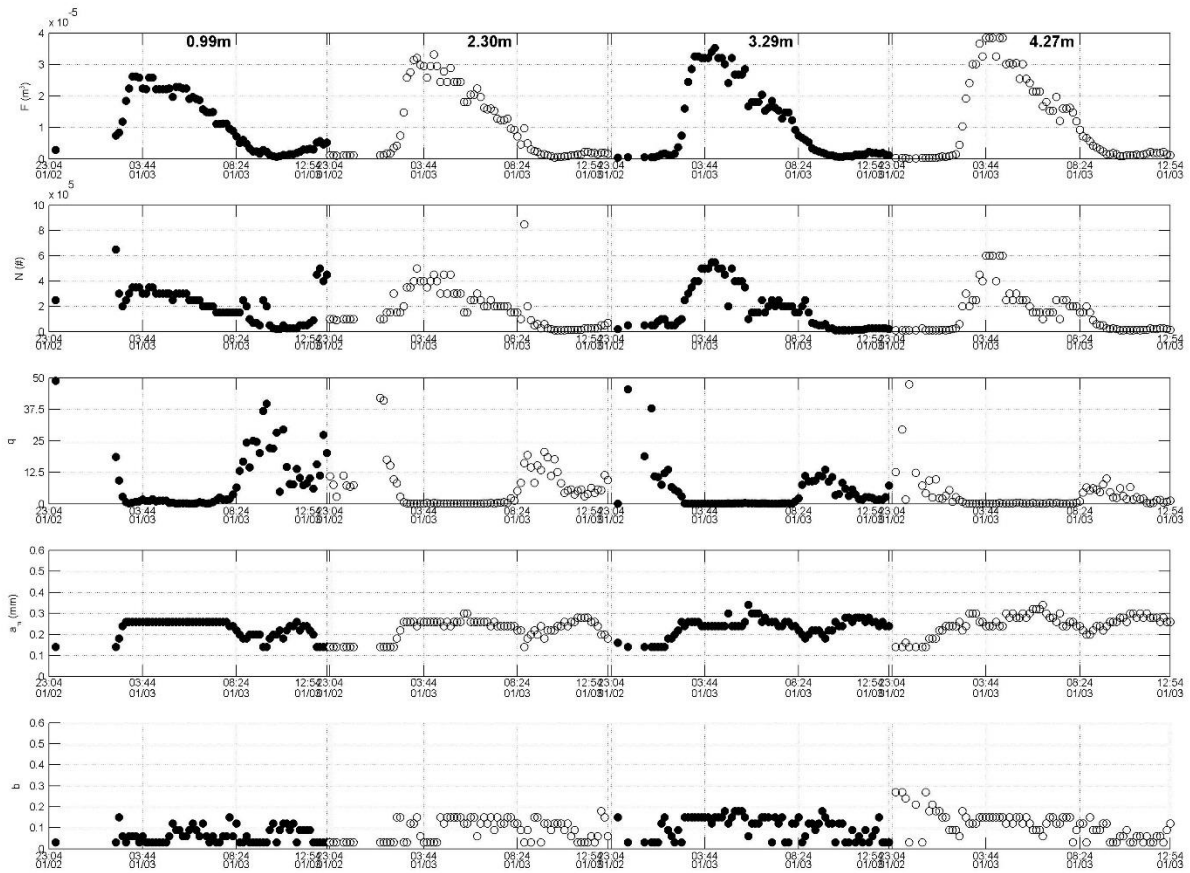


Figure 3b. Plots of extracted and derived parameters corresponding to 10 minute-averaged channels 2-4 data from interval 2. Reading from the top to the bottom of the Figure, the plotted quantities are:  $F$  (fractional volume);  $N$  (particle concentration (particles/m<sup>3</sup>));  $q$  (quality factor);  $a_m$  (median effective radius); and  $b$  (radius spread).

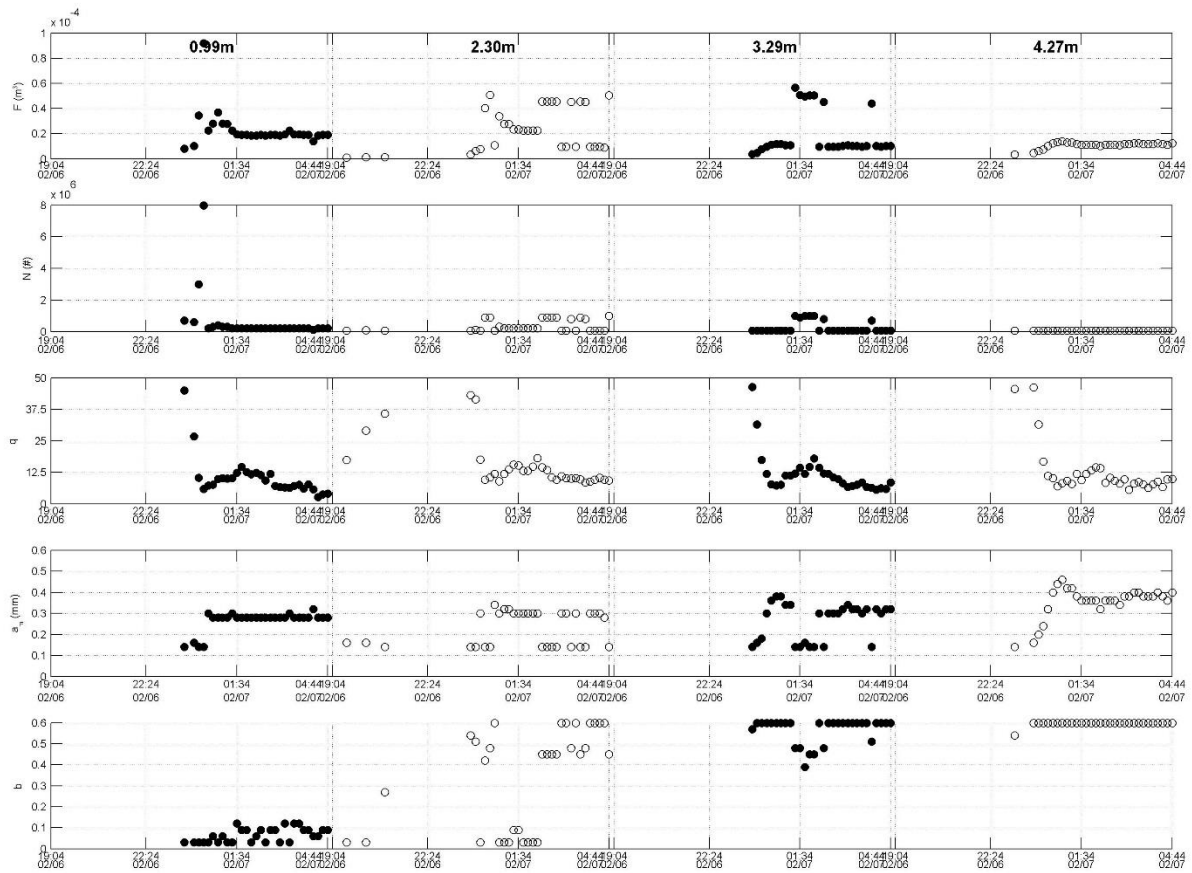


Figure 4a. Plots of extracted and derived parameters corresponding to 10 minute-averaged channels 1-3 data from interval 5. Reading from the top to the bottom of the Figure, the plotted quantities are: F (fractional volume); N (particle concentration (particles/m<sup>3</sup>)); q (quality factor); a<sub>m</sub> (median effective radius); and b (radius spread).

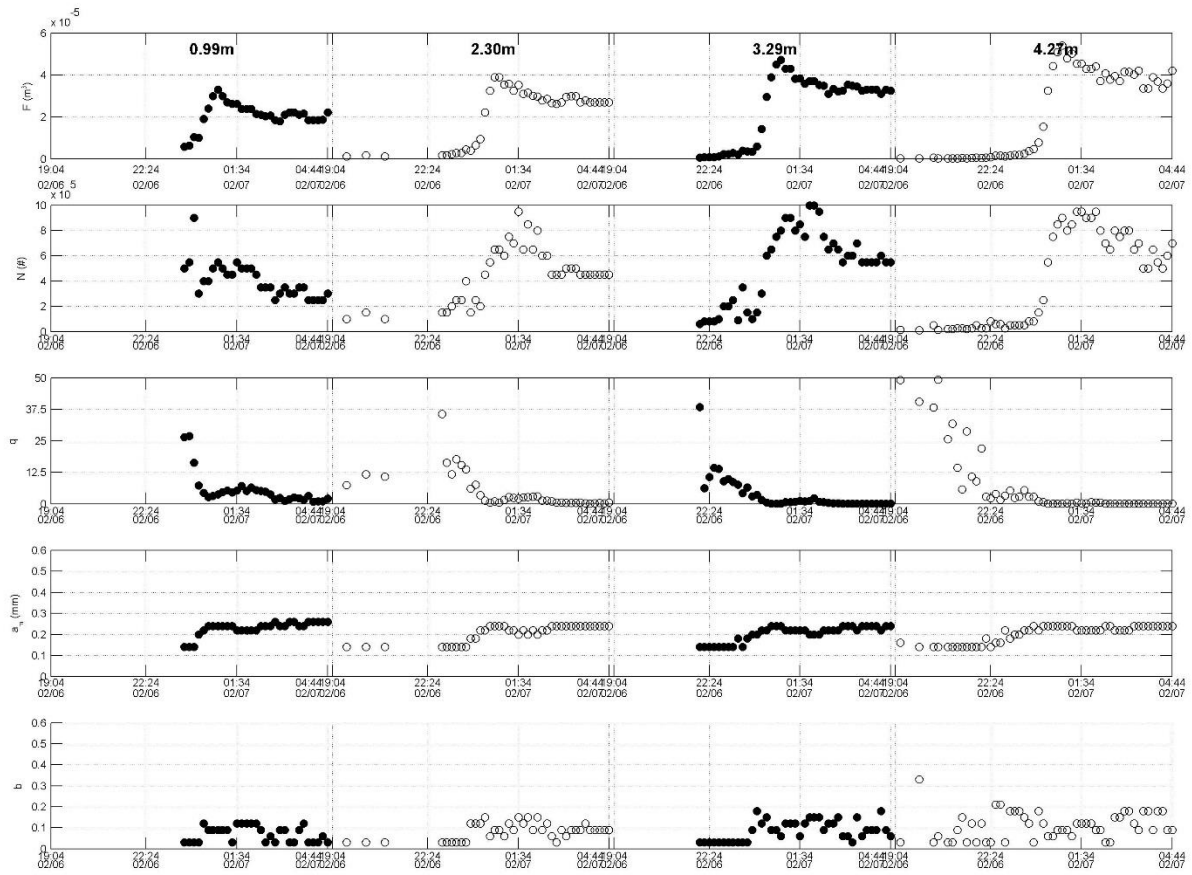


Figure 4b. Plots of extracted and derived parameters corresponding to 10 minute-averaged channels 2-4 data from interval 5. Reading from the top to the bottom of the Figure, the plotted quantities are:  $F$  (fractional volume);  $N$  (particle concentration (particles/m<sup>3</sup>));  $q$  (quality factor);  $a_m$  (median effective radius); and  $b$  (radius spread).

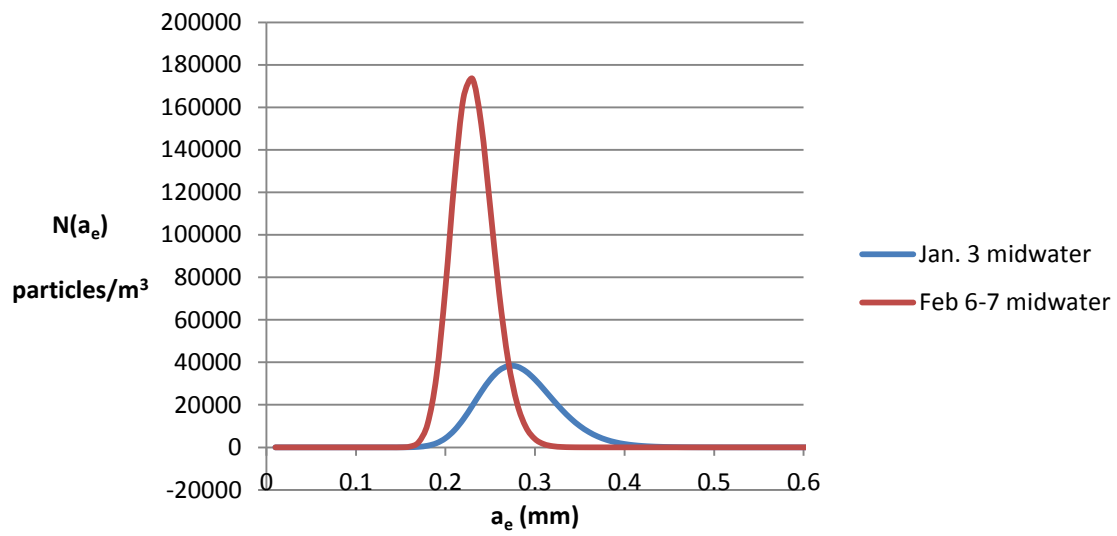


Figure 5. Particle concentrations (particles/m<sup>3</sup>) as a function of effective radius as extracted from interval 2 and 5 (Jan. 2-3 and Feb. 6-7, respectively) channel 2-4 data acquired at range = 2.3m.

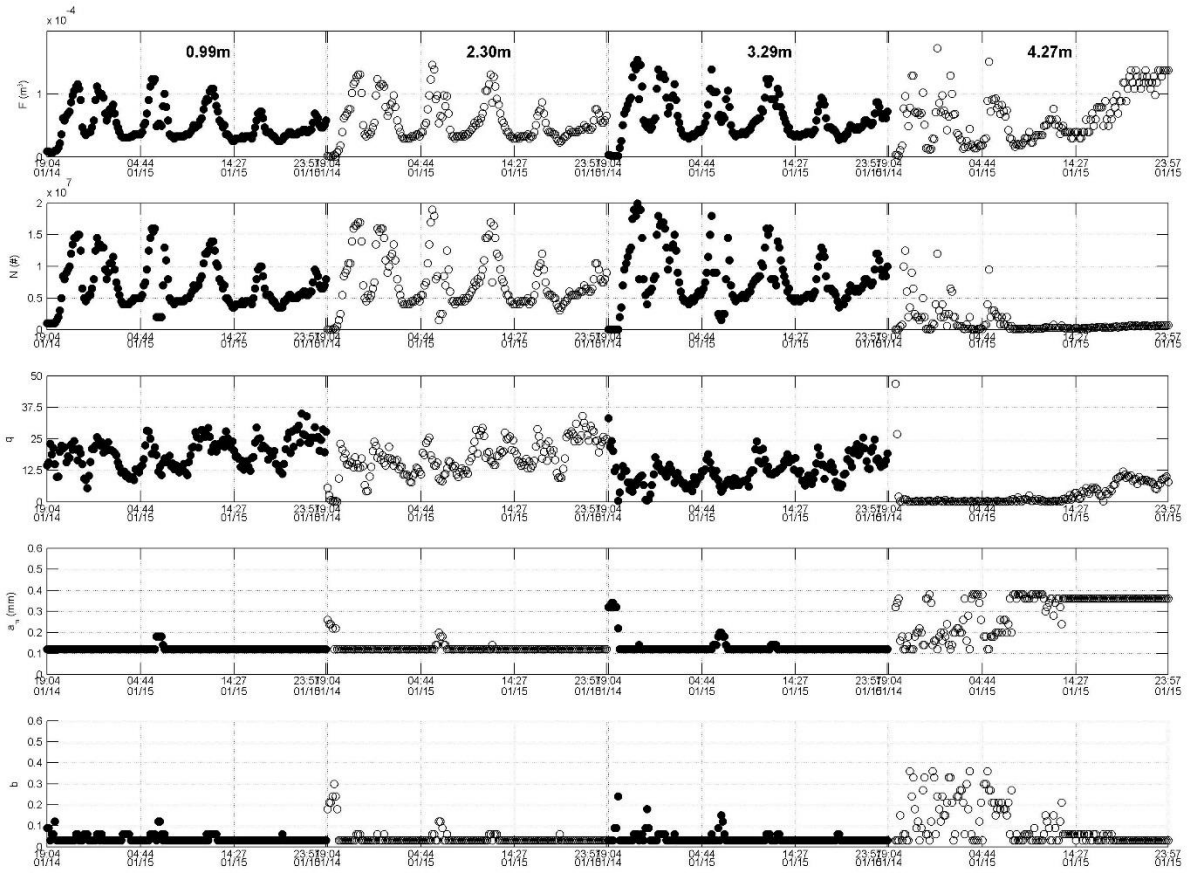


Figure 6. Plots of extracted and derived parameters corresponding to 10 minute-averaged channels 2-4 data from interval 3. Reading from the top to the bottom of the Figure, the plotted quantities are:  $F$  (fractional volume);  $N$  (particle concentration (particles/ $m^3$ ));  $q$  (quality factor);  $a_m$  (median effective radius); and  $b$  (radius spread).



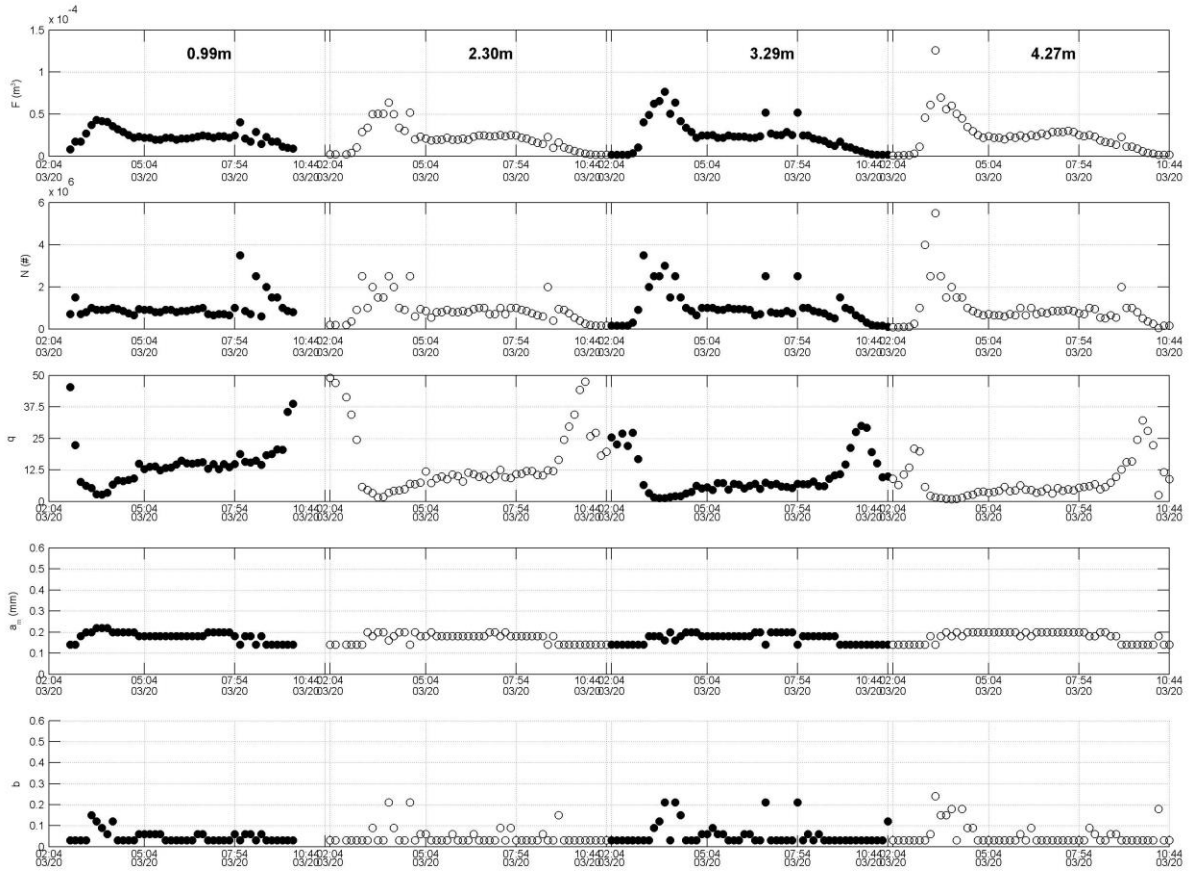


Figure 8. Plots of extracted and derived parameters corresponding to 10 minute-averaged channels 2-4 data from interval 6. Reading from the top to the bottom of the Figure, the plotted quantities are: F (fractional volume); N (particle concentration (particles/m<sup>3</sup>)); q (quality factor);  $a_m$  (median effective radius); and b (radius spread).

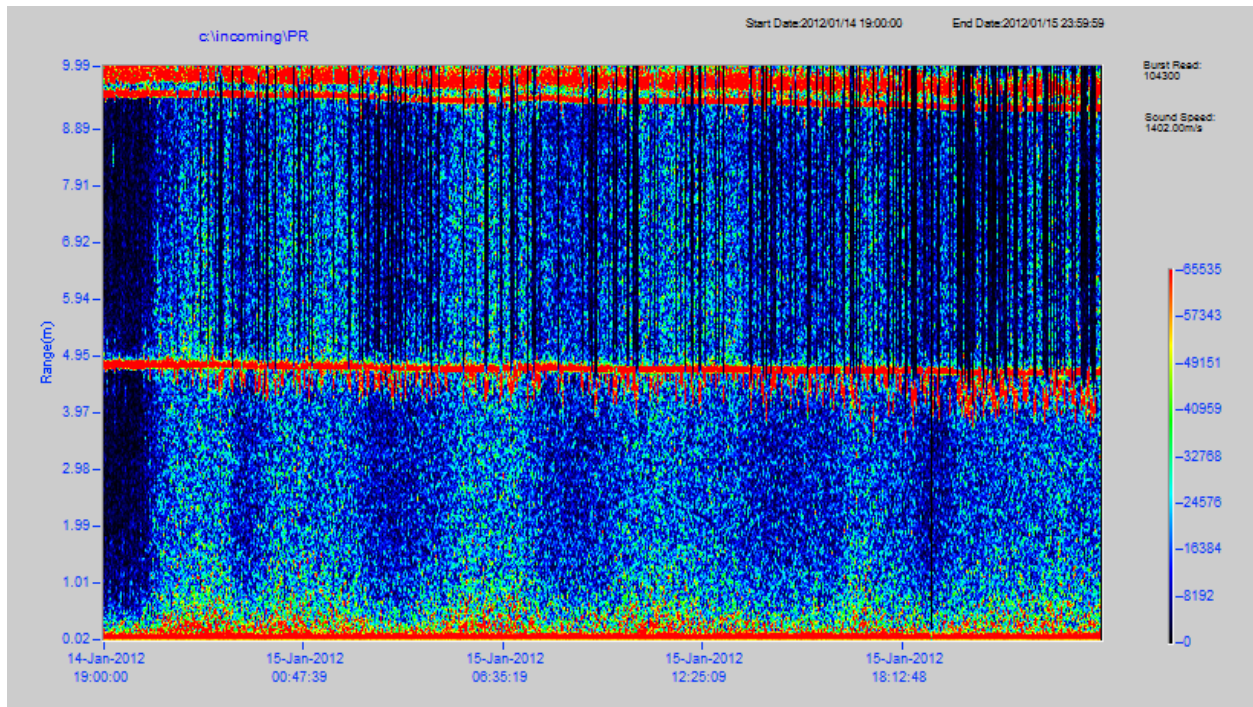


Figure 9. ProfileView plot of channel 4 returns for interval 3.